Diet-Induced Adipose Tissue Inflammation and Liver Steatosis Are Prevented by DPP-4 Inhibition in Diabetic Mice

Jun Shirakawa,[1] Hideki Fujii,[2] Kei Ohnuma,[3] Koichiro Sato,[1] Yuzuru Ito,[1] Mitsuyo Kaji,[1] Eri Sakamoto,[1] Megumi Koganei,[4] Hajime Sasaki,[4] Yoji Nagashima,[5] Kikuko Amo,[6] Kazutaka Aoki,[1] Chikao Morimoto,[3] Eiji Takeda,[6] and Yasuo Terauchi[1]

OBJECTIVE—Diet composition alters the metabolic states of adipocytes and hepatocytes in diabetes. The effects of dipeptidyl peptidase-4 (DPP-4) inhibition on adipose tissue inflammation and fatty liver have been obscure. We investigated the extrapancreatic effects of DPP-4 inhibition on visceral fat and the liver.

RESEARCH DESIGN AND METHODS—We investigated diet-induced metabolic changes in β-cell–specific glucokinase haploinsufficient (*Gck*$^{+/-}$) diabetic mice. We challenged animals with a diet containing a combination of sucrose and oleic acid (SO) or sucrose and linoleic acid (SL). Next, we assessed the effects of a DPP-4 inhibitor, des-fluoro-sitagliptin, on adipose tissue inflammation and hepatic steatosis.

RESULTS—The epididymal fat weight and serum leptin level were significantly higher in *Gck*$^{+/-}$ mice fed SL than in mice fed SO, although no significant differences in body weight or adipocyte size were noted. Compared with SO, SL increased the numbers of CD11c^{+} M1 macrophages and CD8^{+} T-cells in visceral adipose tissue and the expression of E-selectin, P-selectin, and plasminogen activator inhibitor-1 (PAI-1). DPP-4 inhibition significantly prevented adipose tissue infiltration by CD8^{+} T-cells and M1 macrophages and decreased the expression of PAI-1. The production of cytokines by activated T-cells was not affected by DPP-4 inhibition. Furthermore, DPP-4 inhibition prevented fatty liver in both wild-type and *Gck*$^{+/-}$ mice. DPP-4 inhibition also decreased the expressions of sterol regulatory element–binding protein-1c, stearoyl-CoA desaturase-1, and fatty acid synthase, and increased the expression of peroxisome proliferator–activated receptor-α in the liver.

CONCLUSIONS—Our findings indicated that DPP-4 inhibition has extrapancreatic protective effects against diet-induced adipose tissue inflammation and hepatic steatosis. ***Diabetes*** **60:1246–1257, 2011**

From the [1]Department of Endocrinology and Metabolism, Graduate School of Medicine, Yokohama-City University, Yokohama, Japan; the [2]Department of Microbiology and Immunology, Keio University School of Medicine, Tokyo, Japan; the [3]Division of Clinical Immunology, Institute of Medical Sciences, University of Tokyo, Tokyo, Japan; the [4]Food Science Institute, Division of Research and Development, Meiji Dairies Corporation, Odawara, Japan; the [5]Department of Molecular Pathology, Graduate School of Medicine, Yokohama-City University, Yokohama, Japan; and the [6]Department of Clinical Nutrition, Institute of Health Biosciences, Tokushima University, Tokushima, Japan.

Corresponding author: Yasuo Terauchi, terauchi-tky@umin.ac.jp.

Received 20 September 2010 and accepted 27 December 2010.

DOI: 10.2337/db10-1338

This article contains Supplementary Data online at http://diabetes.diabetesjournals.org/lookup/suppl/doi:10.2337/db10-1338/-/DC1.

The prevalence of diabetes and metabolic syndrome has increased dramatically in Western societies and Asia, mainly because of the popularization of high-fat and high-sucrose diets. The combination of high levels of dietary sugars and fatty acids causes metabolic abnormalities in multiple organs (1,2). A hallmark of metabolic syndrome is the expansion of the visceral adipose tissue, which is under a state of chronic inflammation (3). The accumulation of adipose tissue macrophages (ATMs) is thought to be a major component of the chronic inflammatory response (4). Nonalcoholic fatty liver disease (NAFLD) occurs in patients with components of metabolic syndrome. The secretome of chronically inflamed adipose tissue leads to an altered metabolic state with insulin resistance and NAFLD (5).

Sucrose is a major carbohydrate constituent of the diet, and diets rich in sucrose result in hepatic steatosis. Palmitic acid, linoleic acid, and oleic acid are the major fatty acid components of dietary fat and plasma triglycerides (6). Although palmitic acid–induced metabolic abnormalities are well-known, the effects of oleic acid and linoleic acid, two major unsaturated fatty acids, have not been fully elucidated. Hence, we examined two diet protocols to compare dietary oleic acid with linoleic acid (7). Both of these diet protocols contain a similar amount of palmitic acid.

Dipeptidyl peptidase-4 (DPP-4) is responsible for the degradation of numerous peptides and chemokines that contain an alanine or proline at position 2. A DPP-4 inhibitor, des-fluoro-sitagliptin (DFS), acts by inhibiting the breakdown of regulatory peptides including incretins such as glucagon-like peptide-1 (GLP-1) or glucose-dependent insulinotropic polypeptide (GIP) and increasing insulin release (8). However, the clinical benefits of DPP-4 inhibitor therapy cannot be fully explained by the increase in insulin release alone, and other mechanisms are thought to affect β-cell mass, β-cell apoptosis, and other tissues (9–11). Recently, the extrapancreatic actions of GLP-1 on cardiac muscle and endothelial cells have frequently been reported (12). In addition, a GLP-1 receptor agonist exendin-4 improved hepatic steatosis in *ob/ob* mice (13) and the exogenous expression of GLP-1 reduced hepatic gluconeogenesis in *ob/ob* mice (14). Exendin-4 also directly affected human hepatocytes via the GLP-1 receptor (15). Furthermore, exendin-4 inhibited monocyte adhesion to endothelial cells (16) and GLP-1 receptor signaling affected lymphocyte proliferation (17). However, the beneficial effect of DPP-4 inhibition on diet-induced extrapancreatic effects, especially on adipose tissue inflammation, remains poorly understood.

In this study, we used β-cell–specific glucokinase haploinsufficient ($Gck^{+/-}$) mice, which were generated by disrupting the β-cell– and brain-specific exon (18), to evaluate the impact of diet on visceral fat and the liver in the presence of a diabetic state. $Gck^{+/-}$ mice are an animal model of nonobese type 2 diabetes caused by impaired insulin secretion in response to glucose (18,19). Thus, $Gck^{+/-}$ mice manifest hyperglycemia after glucose loading as a result of their impaired insulin secretion, but the gene levels in the liver and adipose tissue are essentially normal. We assumed that, in combination with environmental factors such as an SL diet, high glucose or low insulin levels would induce alterations in the expressions of several genes in the liver as well as the adipose tissue in $Gck^{+/-}$ mice. We then investigated whether a DPP-4 inhibitor can prevent nutrient-induced visceral adipose tissue inflammation and NAFLD.

RESEARCH DESIGN AND METHODS

We backcrossed $Gck^{+/-}$ mice (18) with C57Bl/6 J mice more than 10 times. Both the wild-type and $Gck^{+/-}$ mice were fed standard chow (MF; Oriental Yeast, Japan) until 8 weeks of age and then were given free access to the experimental diets. All the experiments were conducted on male littermates. All the animal procedures were performed in accordance with the institutional animal care guidelines and the guidelines of the Animal Care Committee of the Yokohama City University. The animal housing rooms were maintained at a constant room temperature (25°C) and on a 12-h light (7:00 A.M.)/dark (7:00 P.M.) cycle.

Diets. The experimental diets were freshly prepared weekly. The compositions of the diet containing a combination of sucrose and oleic acid (SO) and the isocaloric diet containing a combination of sucrose and linoleic acid (SL) are shown in Supplementary Table 1. Both diets contained a similar amount of palmitic acid. Wild-type and $Gck^{+/-}$ mice were randomly assigned to one of the two diet groups. The DFS used in this study was prepared by Process Research, Merck Research Laboratories (Rahway, NJ) (8). DFS was administrated orally by premixing with the SL diet to a concentration of 1.1% because this concentration of DFS has been found to result in a 90% inhibition of the plasma DPP-4 activity (20).

Measurement of biochemical parameters and cytokines. Plasma glucose levels, blood insulin levels, and triglyceride content in the liver were determined with a Glutest Neo Super (Sanwa Chemical), insulin kit (Morinaga), and Determiner-L TG II kit (Wako Pure Chemical Industries), respectively. Plasma alanine aminotransferase, free fatty acid, total cholesterol, LDL cholesterol, and triglyceride were assayed by enzymatic methods (Wako Pure Chemical Industries).

Histological analysis. Formalin-fixed, paraffin-embedded adipose tissue sections were immunostained with antibodies to F4/80 (Serotec), CD11c (BD Bioscience), and plasminogen activator inhibitor (PAI)-1 (Santa Cruz). Biotinylated secondary antibodies, a VECTASTAIN elite ABC kit, and a diaminobenzidine substrate kit (VECTOR) were used to examine the sections using bright-field microscopy, and Alexa Fluor 488-, 555-, and 647-conjugated secondary antibodies (Invitrogen) were used for fluorescence microscopy. All the images were acquired using a BZ-9000 microscope (Keyence) or a Carl Zeiss LSM 510 confocal laser scanning microscope. More than five tissue sections from each animal including representative sections of each tissue region were analyzed.

Liver sections were prepared and stained using a Masson-Goldner staining kit (Merck) according to the manufacturer's instructions.

Preparation and flow cytometric analysis of stromal vascular fraction. The adipose stromal vascular fraction (SVF) was prepared by collagenase digestion (Nitta Gelatin) of epididymal fat tissue from each mouse as previously described (21). For flow cytometry, the SVF pellet was resuspended in erythrocyte lysis buffer and incubated in staining medium (PBS with 2% endotoxin-free FBS; 0.1% sodium azide). The cells were incubated with antibodies to CD16/32 (BD Biosciences) to block the Fcγ receptors prior to staining with conjugated antibodies. SVF cells were analyzed for ATMs by staining with antibodies to F4/80 (serotec) and CD11c (BD Bioscience). SVF cells were analyzed for T-cell subsets by staining with antibodies to CD3e, CD4, and CD8 (BD Bioscience), and T-cells were identified by the expression of CD3 and gated for analysis. Flow cytometry was performed using a FACS Canto II (BD Biosciences).

Real-time PCR. Tissue specimens were preserved in RNA*later* reagent (QIAGEN) until the isolation of the total RNA. Total RNA was isolated from the liver tissue using a QIA shredder and an RNeasy kit (QIAGEN). Total RNA was isolated from the epididymal fat using an RNeasy lipid tissue kit (QIAGEN). cDNA was prepared using the Taqman reverse transcriptase kit (Applied Biosystems) and was subjected to quantitative PCR by performing Taqman Gene Expression Assays using the Universal Master Mix (7500 real-time [RT]-PCR system; Applied Biosystems). All probes used in the Taqman Gene Expression Assays were purchased from Applied Biosystems. Each quantitative reaction was performed in duplicate. The data were normalized to the value for β-actin.

Stimulation of T-cells, ELISA, and analysis of intracellular cytokines. $CD4^+$ T-cells and $CD8^+$ T-cells were separated from splenocyte of wild-type or $Gck^{+/-}$ mice by negative and positive selection using auto magnetic cell sorting as previously described (22). The purity of each cell was >90% as analyzed by flow cytometry. Cells (2×10^5 cells/well) were stimulated with plate-coated anti-CD3 and anti-CD28 monoclonal antibodies in a total volume of 0.5 mL in 96-well round bottom plates. T-cells were expanded and maintained in the same culture conditions for 3 days.

For antigen-presenting cell (APC) preparation, $CD11c^+$ splenocytes from wild-type C57BL/6 mice were cultured at 1×10^5 cells/well in a 96-well round-bottom plate with 1 μg/mL soluble ovalbumin. Splenocytes from homozygous OT-I TCR-Tg and OT-II TCR-Tg C57BL/6 mice (The Jackson Laboratory) were prepared and stimulated with APCs at 1×10^5 cells/well in a 96-well round-bottom plate for 3 days.

Exendin-4 was added to culture medium at a concentration of 100 nmol/L. DFS was added to culture medium at a concentration of 1 μmol/L or 100 μmol/L. Recombinant soluble human CD26 (rsCD26) (23) was added to culture medium at a concentration of 0.5 mg/mL.

Concentrations of γ-interferon (IFN-γ), tumor necrosis factor (TNF)-α, monocyte chemoattractant protein (MCP)-1, and interleukin (IL)-10 in culture supernatants were determined using an ELISA kit (R&D systems) according to the manufacturer's instructions. Intracellular IFN-γ, TNF-α, and MCP-1 synthesis was analyzed by flow cytometry by using a BD Cytofix/Cytoperm Fixation/Permealization kit with BD GolgiPlug (BD Biosciences) according to the manufacturer's instructions.

Statistical analyses. All the data were reported as means ± SE and analyzed using Student *t* test or ANOVAs. Differences were considered significant if the *P* value was <0.05.

RESULTS

SL induced adipose tissue hypertrophy but did not affect body weight in $Gck^{+/-}$ mice. Wild-type mice and $Gck^{+/-}$ mice fed an SO diet or an isocaloric SL diet for 25 weeks were evaluated for blood glucose level, body weight, liver weight, and epididymal fat weight (Fig. 1*A*). No significant differences in body weight, liver weight, blood glucose level, or serum insulin concentration were observed between the SO group and the SL group of either genotype (Table 1). However, the ratio of the epididymal fat weight to the body weight of SL-fed $Gck^{+/-}$ mice was significantly higher than that of SO-fed $Gck^{+/-}$ mice despite a similar body weight. In wild-type mice, no differences in the epididymal fat weight were observed between the SO group and the SL group. The body weight gain and the food intake of both the wild-type and the $Gck^{+/-}$ mice fed either the SO diet or the SL diet were similar to those of animals fed a standard chow diet; however, the fasting blood glucose levels were significantly higher among animals fed a standard chow diet in both the wild-type and the $Gck^{+/-}$ mice (Supplementary Table 2). Among the $Gck^{+/-}$ mice, the SL diet decreased insulin secretion at 15 min after oral glucose loading compared with the SO diet but did not affect insulin sensitivity after an insulin injection (Fig. 1*B–D*). No significant differences in the serum lipid parameters were observed among the four groups (Supplementary Fig. 1). These results indicated that the SL diet induced visceral adipose tissue hypertrophy under diabetic conditions.

SL recruited M1 macrophages to visceral fat and increased the expression of PAI-1 in $Gck^{+/-}$ mice. Both the wild-type and the $Gck^{+/-}$ mice fed either the SO or the SL diet displayed a similar adipocyte size and

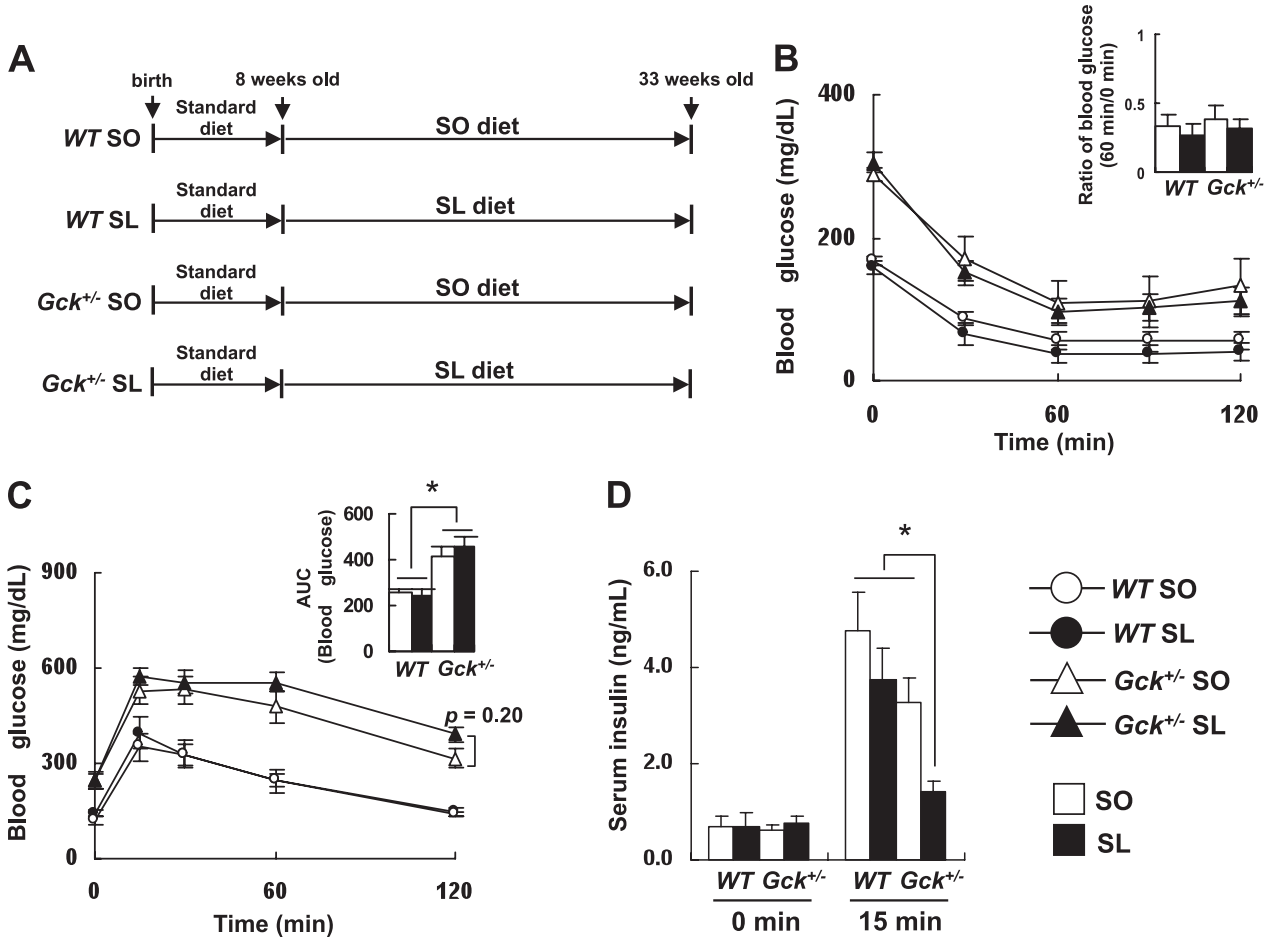

FIG. 1. SL-induced impaired insulin secretion in $Gck^{+/-}$ mice. *A*: Experimental protocol. Both the wild-type (*WT*) and $Gck^{+/-}$ mice were fed standard chow diet until 8 weeks of age and then given free access to the experimental diets. Experiments were performed on wild-type and $Gck^{+/-}$ mice after 25 weeks on the SO (□) or SL (■) diet. *B*: Insulin tolerance (n = 10–12). *C* and *D*: Glucose tolerance (n = 10–12). *C*: Plasma glucose levels. ○, wild-type mice on SO diet; ●, wild-type mice on SL diet; △, $Gck^{+/-}$ mice on SO diet; ▲, $Gck^{+/-}$ mice on SL diet. *D*: Serum insulin levels. *$P < 0.05$.

serum concentration of adiponectin (Fig. 2*A* and *C*). The adipocyte area in all four groups was larger than in the standard diet–fed mice but smaller than that in the high-fat diet (HFD32)-fed mice (Supplementary Fig. 2). Consistent with visceral fat hypertrophy in the $Gck^{+/-}$ mice fed the SL diet, the serum leptin concentration was also significantly increased (Fig. 2*B*).

An immunohistochemical analysis showed a significant increase in F4/80$^+$ crown-like structures (CLSs) in $Gck^{+/-}$ mice fed the SL diet compared with $Gck^{+/-}$ mice fed the SO diet (Fig. 2*D* and *E*). F4/80$^+$ CLSs were hardly detected in the epididymal adipose tissue of the wild-type and the $Gck^{+/-}$ mice fed a standard diet (Supplementary Fig. 3). A phenotypic switch of ATMs from an anti-inflammatory M2 polarization state to a proinflammatory M1 polarization state is thought to be responsible for the inflammatory changes in the adipose tissue (21,24). The total numbers of nucleated cells and CD11c$^+$ CLSs were also higher among the $Gck^{+/-}$ mice fed the SL diet than among the $Gck^{+/-}$ mice fed the SO diet (Fig. 2*F*). In the wild-type mice, no significant differences in the number of F4/80$^+$ CLSs and CD11C$^+$ CLSs observed in the epididymal fat were seen between the SO group and the SL group. Because the production of PAI-1 by ATMs was reported to be a response to a nutritional signal (free fatty acid [FFA]) (25), we examined the PAI-1 expression level in epididymal fat. The expression of PAI-1 was enhanced surrounding CD11C$^+$ CLSs in the $Gck^{+/-}$ mice fed the SL diet (Fig. 2*G*). The mRNA expression levels of F4/80, CD11c, and PAI-1 were significantly higher among the $Gck^{+/-}$ mice fed the SL diet than among the $Gck^{+/-}$ mice fed the SO diet (Fig. 2*H*).

SL induced adipose tissue inflammation, infiltration of CD8$^+$ T-cells, and expression of E-selectin and P-selectin in $Gck^{+/-}$ mice. Next, we isolated the SVF of cells from the epididymal fat pads of wild-type and $Gck^{+/-}$ mice fed either the SO or the SL diet and analyzed them using flow cytometry. The proportion of F4/80$^+$ ATMs was significantly higher in the SVF cells of the $Gck^{+/-}$ mice fed the SL diet than in those of the mice fed the SO diet (Fig. 3*A*). The proportion of F4/80$^+$ CD11c$^+$ cells among the F4/80$^+$ ATMs was also higher in the SL group (Fig. 3*B* and *C*). CD4$^+$ and CD8$^+$ T-cells have recently been reported to play crucial roles in the initiation and propagation of adipose inflammation by promoting the recruitment and activation of macrophages in adipose tissue (26–28). The proportion of the CD4$^+$ subset and the CD8$^+$ subset among the SVF CD3$^+$ T-cells was investigated using flow cytometry. The proportion of the CD8$^+$ T-cell subset was significantly higher among the $Gck^{+/-}$ mice fed the SL diet (Fig. 3*D* and *E*). No significant differences in the SVF cells

TABLE 1
Effects of experimental diets at week 25 on body weight, liver weight, epididymal fat weight, blood glucose level, and serum insulin concentration after a 16-h fast in wild-type and *Gck*$^{+/-}$ mice

	Wild-type		*Gck*$^{+/-}$	
	SO	SL	SO	SL
Body weight (g)	41.00 ± 2.39	39.67 ± 2.39	40.67 ± 2.38	41.60 ± 1.61
Liver weight (g)	1.87 ± 0.20	1.67 ± 0.15	2.43 ± 0.34	1.87 ± 0.15
Epididymal fat weight (g)	0.98 ± 0.15	0.89 ± 0.26	1.18 ± 0.19	1.74 ± 0.21
Liver weight/body weight (%)	4.55 ± 0.40	4.21 ± 0.28	5.87 ± 0.51*	4.48 ± 0.25
Epididymal fat weight/body weight (%)	2.36 ± 0.29	2.15 ± 0.58	2.86 ± 0.35	4.24 ± 0.60†
Glucose (mg/dL)	114 ± 3‡	110 ± 4‡	178 ± 9	181 ± 6
Insulin (ng/mL)	0.68 ± 0.038	0.65 ± 0.048	0.69 ± 0.036	0.76 ± 0.059

Data are means ± SE. n = 8–10. *$P < 0.05$ relative to wild-type SL and *Gck*$^{+/-}$ SL. †$P < 0.05$ relative to wild-type SO, wild-type SL, and *Gck*$^{+/-}$ SO. ‡$P < 0.05$ relative to *Gck*$^{+/-}$ SO and *Gck*$^{+/-}$ SL.

of the wild-type mice were observed. No significant changes in the subsets of splenic T-cells were observed in any of the groups (Supplementary Fig. 4). Because the expressions of E-selectin and P-selectin were reportedly enhanced in the SVF of inflamed adipose tissue from obese animals (29), we measured the level of TNF-α, MCP-1, E-selectin, and P-selectin expression in the epididymal fat tissue using RT-PCR. The mRNA expression levels of TNF-α and MCP-1 tended to be higher in the *Gck*$^{+/-}$ mice fed the SL diet than in the *Gck*$^{+/-}$ mice fed the SO diet (Fig. 3*F*). The expressions of E-selectin and P-selectin in the epididymal fat of the wild-type and *Gck*$^{+/-}$ mice fed the SL diet were significantly higher than those of the wild-type and *Gck*$^{+/-}$ mice fed the SO diet. However, no significant differences in the serum concentrations of TNF-α or MCP-1 were observed between the mouse groups fed the SL diet and those fed the SO diet (Fig. 3*G* and *H*).

DFS ameliorated SL-induced adipose tissue hypertrophy in *Gck*$^{+/-}$ mice. To evaluate DFS as a treatment for diet-induced adipose tissue inflammation, we performed a 20-week study comparing wild-type or *Gck*$^{+/-}$ mice fed a diet consisting of SL or SL plus 1.1% DFS (Fig. 4*A*). The epididymal fat weight and the body weight of the SL-fed *Gck*$^{+/-}$ mice tended to be decreased by the addition of DFS to the diet (Table 2). These body weight changes were observed only after week 17. No significant differences in the liver weight or the fasting serum insulin concentration were observed between the SL group and SL plus DFS group of either genotype. We noted that in *Gck*$^{+/-}$ mice, DFS improved the glucose tolerance and increased the serum insulin level after glucose loading but did not affect insulin sensitivity after an insulin injection (Fig. 4*B-D*). No significant differences in the serum lipid parameters were observed among the four groups after chronic DPP-4 inhibition (Supplementary Fig. 5). These results indicated that DFS prevented SL-induced visceral adipose tissue hypertrophy under diabetic conditions.

DFS prevented the SL-induced recruitment of M1 macrophages to visceral fat by reducing the expression of PAI-1 in *Gck*$^{+/-}$ mice. Next, we analyzed the epididymal fat pads of wild-type and *Gck*$^{+/-}$ mice fed the SL or the SL plus DFS diet for 20 weeks. The adipocyte area tended to be slightly decreased in the DFS groups, but the serum adiponectin levels were unaffected (Fig. 5*A* and *C* and Supplementary Fig. 6). In accordance with the reduced epididymal fat weight, the serum leptin level of the SL-fed *Gck*$^{+/-}$ mice tended to be decreased by DFS (Fig. 5*B*). DFS reduced the number of F4/80$^+$ CLSs (Fig. 5*D* and *E*), the total nucleated cells, and CD11c$^+$ CLSs in the adipose tissue of SL fed-*Gck*$^{+/-}$ mice (Fig. 5*F*). In wild-type mice, no significant differences in F4/80$^+$ CLSs and CD11C$^+$ CLSs of the epididymal fat were observed by the administration of DFS. The expression of PAI-1 around CD11c$^+$ CLSs was also suppressed by DFS (Fig. 5*G*). The mRNA expression analysis also showed that DFS reduced the expressions of F4/80, CD11c, and PAI-1 in *Gck*$^{+/-}$ mice (Fig. 5*H*). Thus, adipose tissue infiltration by M1 macrophages was prevented by DPP-4 inhibition in a diabetic state.

We also conducted experiments using an SO plus DFS diet. DFS did not affect the epididymal fat weight or the number of F4/80$^+$ CLSs in wild-type and *Gck*$^{+/-}$ mice fed the SO diet (data not shown).

DFS protected against SL-induced adipose tissue infiltration by CD8$^+$ T-cells but had no impact on the production of inflammatory cytokines by T-cells. Flow cytometric analyses revealed that DFS significantly prevented the SL-induced increases in the ratios of F4/80$^+$ ATMs (Fig. 6*A*) and F4/80$^+$ CD11c$^+$ cells (Fig. 6*B* and *C*) among the F4/80$^+$ ATMs in the SL-fed *Gck*$^{+/-}$ mice. The ratio of CD8$^+$ subset cells among the CD3$^+$ SVF T-cells in the SL-fed *Gck*$^{+/-}$ mice was significantly reduced to a level similar to that seen in the SO-diet group (Fig. 6*D* and *E*). The mRNA expression levels of TNF-α and MCP-1 were reduced by DFS in *Gck*$^{+/-}$ mice fed the SL diet, but the difference was not significant in TNF-α (Fig. 6*F*). The levels of E-selectin and P-selectin expression were not affected by DFS in any of the mouse groups (Fig. 6*F*). No significant differences in the serum concentrations of TNF-α and MCP-1 were observed between the mouse group fed the SL diet and the group fed the SL-plus-DFS diet (Fig. 6*G* and *H*).

We also investigated the role of DPP-4 inhibition on T-cell–mediated adipose tissue inflammation in vivo. Murine CD26/DPP-4 (mCD26) was expressed on the surface of both CD4$^+$ and CD8$^+$ T-cells, and the expression of mCD26 was upregulated 24 h after transient stimulation (Supplementary Fig. 8). Neither DFS nor exendin-4 affected the production of IFN-γ, TNF-α, MCP-1, or IL-10 by CD4$^+$ or CD8$^+$ T-cells from wild-type and *Gck*$^{+/-}$ mice after stimulation with anti-CD3 and anti-CD28 antibodies (Supplementary Fig. 9). Intracellular cytokine staining also showed no significant differences in IFN-γ, TNF-α, or MCP-1 synthesis (Supplementary Fig. 10). In human peripheral blood cells, exogenous recombinant soluble CD26 (rsCD26) was able to upregulate the CD86 expression on monocytes and enhance the antigen-specific T-cell activation via

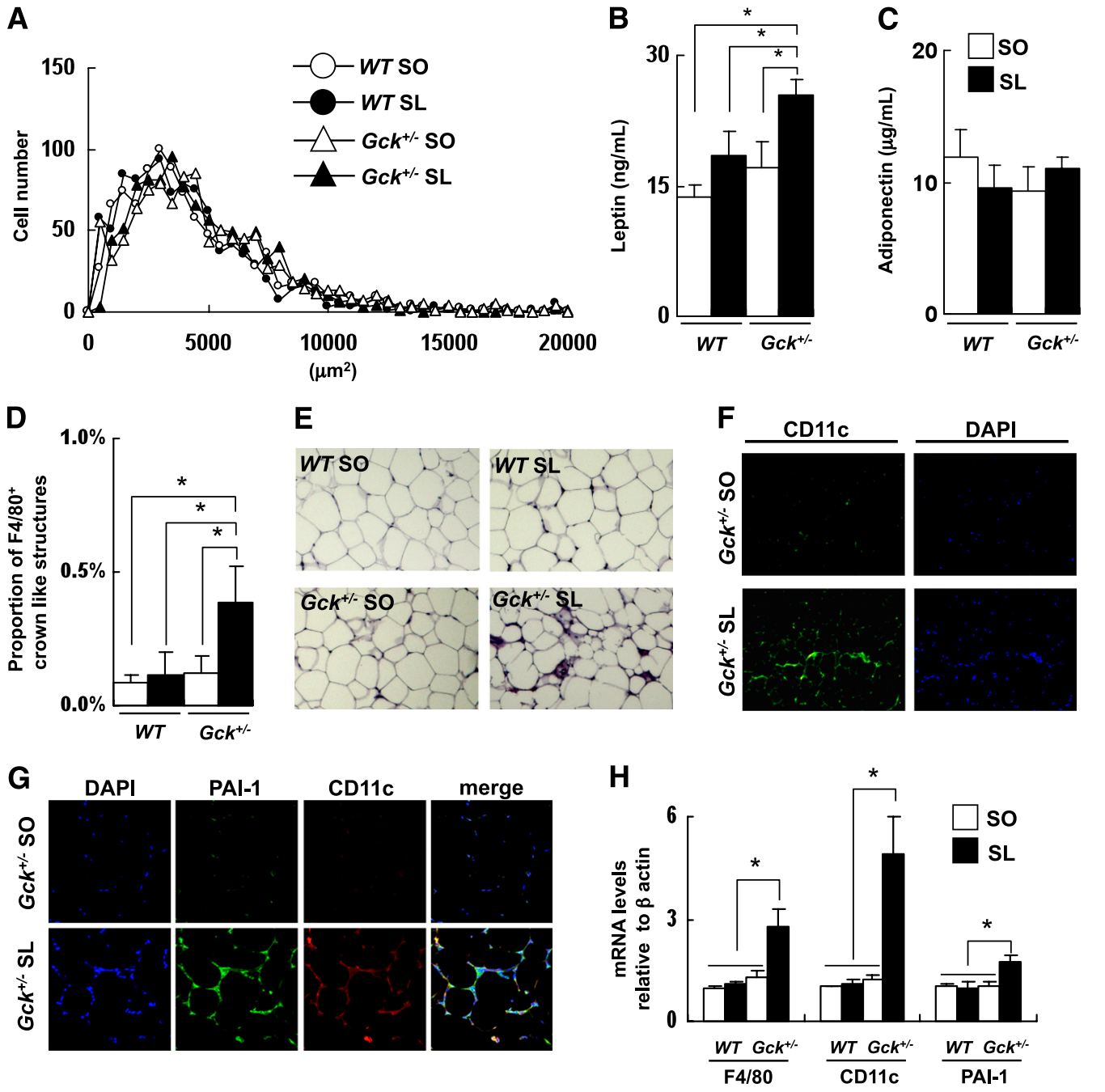

FIG. 2. SL-induced infiltration of adipose tissue by M1 macrophages and expression of PAI-1. *A*: Histogram of adipocyte size of the epididymal fat ($n = 5$). *B* and *C*: Serum leptin and adiponectin levels ($n = 6$–8). *D* and *E*: Epididymal fat tissue was stained with anti-F4/80 antibody. The number of CLSs was counted as described in RESEARCH DESIGN AND METHODS ($n = 5$). *F*: Epididymal fat tissue was stained with anti-CD11c antibody and DAPI. *G*: Epididymal fat tissue was stained with anti–PAI-1 antibody and anti-CD11c antibody. *H*: Assessment of the level of expression of the mRNAs indicated in epididymal fat as determined by real-time quantitative RT-PCR and normalization to the β-actin mRNA level ($n = 5$). Experiments were performed on wild-type (*WT*) and *Gck*$^{+/-}$ mice after 25 weeks on the SO or SL diet. *$P < 0.05$. (A high-quality digital representation of this figure is available in the online issue.)

caveolin-1 (23,30,31). No significant changes in the production of IFN-γ, TNF-α, MCP-1, or IL-10 by the CD4$^+$ T-cells of OT-II mice or the CD8$^+$ T-cells of OT-I mice were observed after stimulation with a specific antigen (ovalbumin peptide) presented by CD11c$^+$ splenic APCs in the presence of DFS, exendin-4, or rsCD26 (Supplementary Fig. 11).

DFS protected against diet-induced hepatic steatosis. Diets containing a large amount of sucrose reportedly resulted in fatty liver in mice (32,33). In the current study, we fed a sucrose-rich diet (36% sucrose diet) to wild-type and *Gck*$^{+/-}$ mice and investigated the severity of steatosis in the four groups. Mild steatosis occurred in the livers of all the groups, but evidence of inflammatory cell infiltration of the liver was not seen in any of the groups (Supplementary Fig. 12*A*). By contrast, steatosis was not observed in wild-type or *Gck*$^{+/-}$ mice of the same age fed a standard diet (Supplementary Fig. 13*A*). When hepatic steatosis was graded from 1 to 3, as shown in Supplementary Fig. 14 (34), no significant differences in the grade of steatosis were found among the four groups

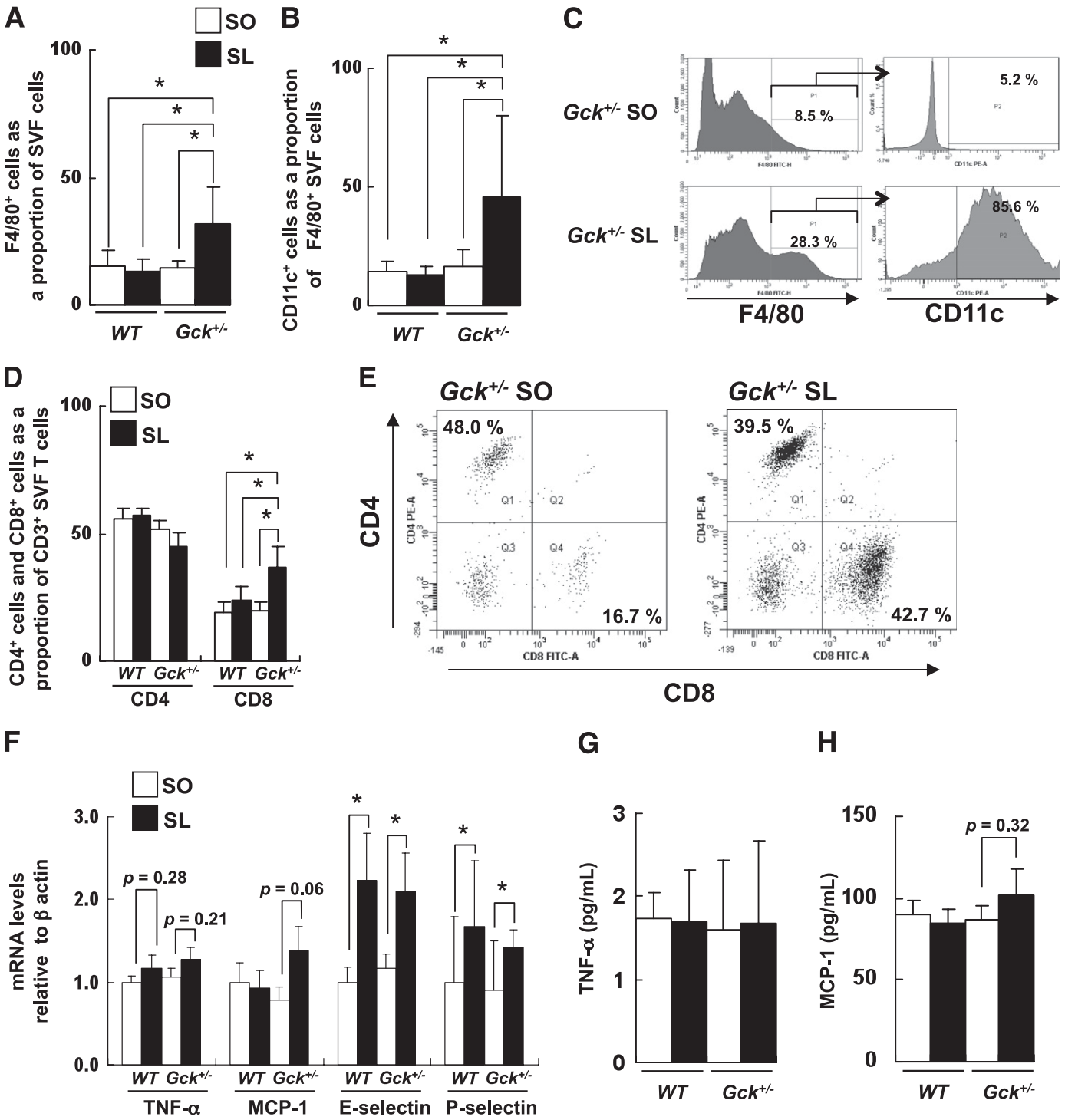

FIG. 3. SL-induced adipose tissue inflammation by infiltration of CD11c$^+$ M1 macrophages and CD8$^+$ T-cells. *A*: Number of F4/80$^+$ cells as a proportion of the cells in the SVF of epididymal fat from the mice as determined by flow cytometry (n = 5). *B*: Number of CD11c$^+$ cells as a proportion of the F4/80$^+$ cells in the SVF of epididymal fat from the groups of mice indicated as determined by flow cytometry (n = 5). *C*: Flow cytometric analysis of CD11c$^+$ cells among F4/80$^+$ SVF cells from the epididymal fat of *Gck*$^{+/-}$ mice. *D* and *E*: Flow cytometric analysis of the CD4$^+$ subset and CD8$^+$ subset of CD3$^+$ T-cells in the epididymal fat of the groups of mice indicated (n = 5). *F*: Assessment of the level of expression of the mRNAs indicated in epididymal fat as determined by real-time quantitative RT-PCR and normalization to the β-actin mRNA level (n = 5). *G* and *H*: Serum TNF-α and MCP-1 levels (n = 6–8). Experiments were performed on wild-type (*WT*) and *Gck*$^{+/-}$ mice after 25 weeks on the SO or SL diet. *P < 0.05.

(Supplementary Fig. 12*B*). The triglyceride content of the liver and the mRNA expression levels of sterol regulatory element–binding protein (SREBP)-1c, stearoyl-CoA desaturase (SCD)-1, peroxisome proliferator–activated receptor (PPAR)α, SREBP-2, fatty acid synthase (FAS), and TNF-α were similar in all four groups (Supplementary Fig. 12*C* and *D*). The hepatic expressions of phosphoenolpyruvate carboxykinase (PEPCK) and glucose-6-phosphatase (G6Pase) were significantly increased in mice fed a diet of SO or SL, compared with mice fed a standard diet (Supplementary

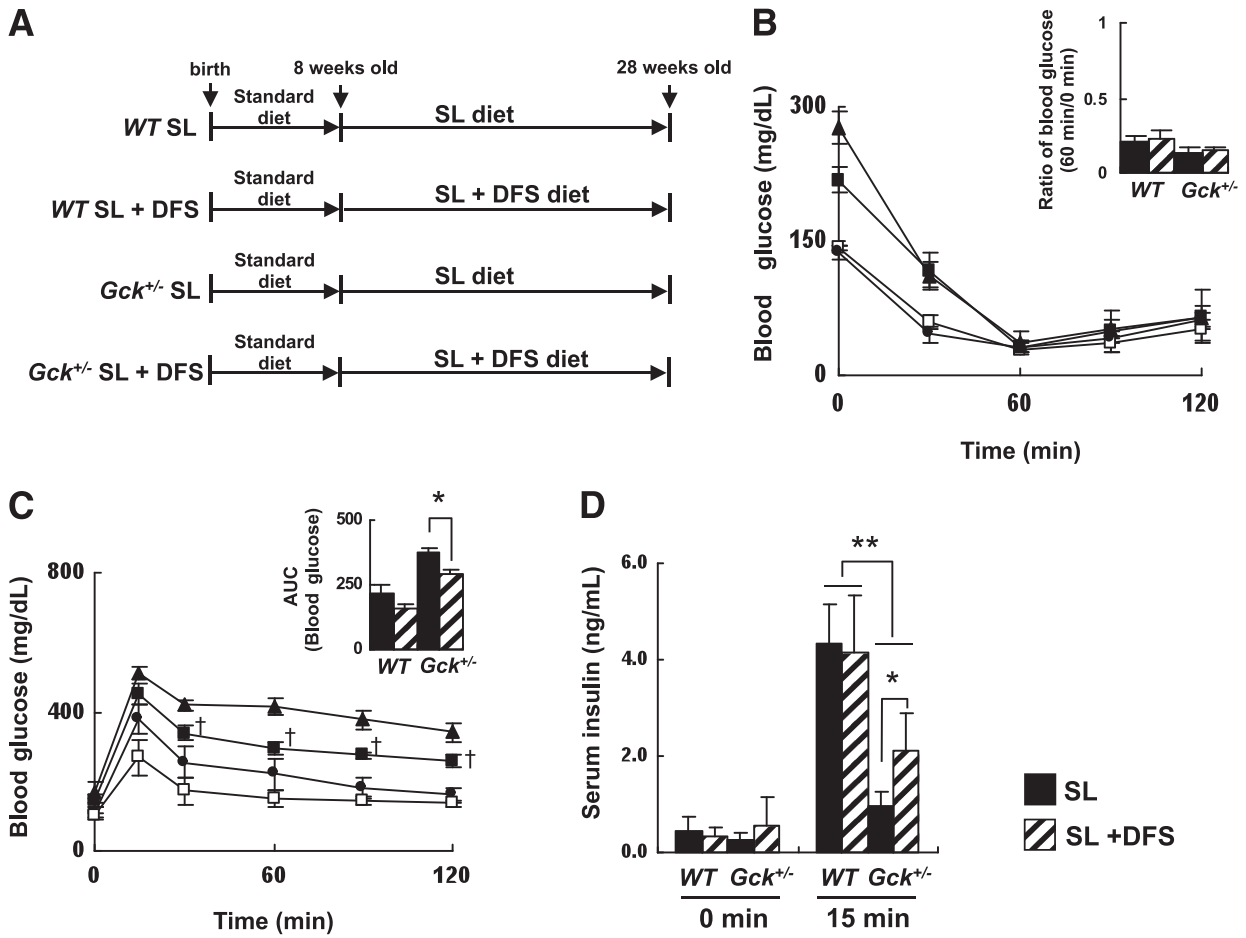

FIG. 4. DFS improved glucose tolerance and insulin secretion in SL diet–fed Gck$^{+/-}$ mice. *A*: Experimental protocol. Both the wild-type and Gck$^{+/-}$ mice were fed standard chow until 8 weeks of age and then given free access to the experimental diets. Experiments were performed on wild-type (*WT*) and *Gck*$^{+/-}$ mice after 20 weeks on the SL or the SL-plus-DFS diet. *B*: Insulin tolerance (n = 9–10). *C* and *D*: Glucose tolerance (n = 9–10). *C*: Plasma glucose levels. ●, wild-type SL mice; □, wild-type SL-plus-DFS mice; ▲, Gck$^{+/-}$ SL mice; ■, Gck$^{+/-}$ SL-plus-DFS mice. AUC, area under the curve. *D*: Serum insulin levels. *P < 0.05. **P < 0.01. †P < 0.05 vs. *Gck*$^{+/-}$ SL.

Fig. 12*E*). We also conducted similar experiments using palatinose, a slowly digestible sucrose analog, instead of sucrose and an oleic acid diet (PO) for 25 weeks. Steatosis was not observed in the wild-type or the *Gck*$^{+/-}$ mice fed the PO diet (Supplementary Fig. 13*B*).

Next, we investigated the effects of DFS on diet-induced fatty liver in wild-type and *Gck*$^{+/-}$ mice fed the SL diet. DFS did not significantly affect the liver weight (Table 2). DFS monotherapy improved steatosis histochemically and significantly decreased the grade of steatosis in both euglycemic wild-type and hyperglycemic *Gck*$^{+/-}$ mice (Fig. 7*A* and *B*). The hepatic triglyceride content was also reduced by treatment with DFS (Fig. 7*C*), and the mRNA expression levels of SREBP-1c, SCD-1, and FAS were decreased and the expression of PPARα was increased by DFS monotherapy in both genotypes (Fig. 7*D*). Furthermore, the administration of DFS reduced the hepatic expression of PEPCK or G6Pase (Fig. 7*E*). DFS also ameliorated fatty liver in wild-type and *Gck*$^{+/-}$ mice fed the SO diet (Supplementary Fig. 13*C*).

DISCUSSION

Adipose tissue has been shown to be a central driver of type 2 diabetes progression, establishing and maintaining a chronic state of low-level inflammation (35). Chronic exposure to high concentrations of glucose and free fatty acids in the blood affects pancreatic β-cell function, lipid synthesis in the liver, and lipid storage in adipose tissue. We here established a nonobese model of diet-induced adipose tissue inflammation and NAFLD in *Gck*$^{+/-}$ mice by feeding them an SL diet. In wild-type mice, no differences in epididymal fat weight were observed between the SO and the SL groups. The body weight gain and food intake of both the wild-type and the *Gck*$^{+/-}$ mice fed either the SO or the SL diet were similar to those of animals fed a standard chow diet. Adipocyte hypertrophy and increased inflammatory cytokines were not observed in this model, and insulin sensitivity was essentially unaffected. The blood glucose levels after insulin injection were found to be lower in mice fed the SO or the SL diet than in mice fed the standard chow diet (data not shown). This finding is consistent with that of a previous report indicating that the blood glucose levels after insulin injection in the high-sucrose diet–fed mice were lower than those in mice fed the standard diet (36). However, the existence of hepatic insulin resistance was suggested by the increased expression of PEPCK and G6Pase in the liver. Similar to human type 2 diabetes, the pathogenic mechanisms underlying this model have a genetic basis (*Gck*$^{+/-}$), yet they also depend more on environmental factors (diet).

TABLE 2
Effects of DFS at week 20 on body weight, liver weight, epididymal fat weight, blood glucose level, and serum insulin concentration after a 16-h fast in wild-type and *Gck*$^{+/-}$ mice

	Wild-type		*Gck*$^{+/-}$	
	SL	SL + DFS	SL	SL + DFS
Body weight (g)	37.26 ± 2.63	35.36 ± 2.49	38.73 ± 1.79*	34.61 ± 0.85
Liver weight (g)	1.75 ± 0.14	1.64 ± 0.09	1.81 ± 0.20	1.46 ± 0.22
Epididymal fat weight (g)	0.98 ± 0.25	0.81 ± 0.12	1.54 ± 0.23*	0.93 ± 0.19
Liver weight/body weight (%)	4.79 ± 0.53	4.75 ± 0.52	4.65 ± 0.40	4.17 ± 0.55
Epididymal fat weight/body weight (%)	2.57 ± 0.58	2.58 ± 0.39	4.17 ± 0.54	2.65 ± 0.51
Glucose (mg/dL)	114 ± 8†	99 ± 5†	162 ± 9	142 ± 6
Insulin (ng/mL)	0.52 ± 0.057	0.57 ± 0.028	0.57 ± 0.055	0.61 ± 0.047

Data are means ± SE. n = 6–10. DFS reduced body weight by 5.1% in wild-type mice and by 10.6% in *Gck*$^{+/-}$ mice, although the reduction was not statistically significant in wild-type mice. *$P < 0.05$ relative to wild-type SL, wild-type SL + DFS, and *Gck*$^{+/-}$ SL + DFS. †$P < 0.05$ relative to *Gck*$^{+/-}$ SL and *Gck*$^{+/-}$ SL + DFS.

In this study, similar levels of body weight, FFA, cholesterol, and triglyceride were observed in the wild-type and *Gck*$^{+/-}$ mice fed the SO and SL diets, suggesting that the adipose tissue inflammation induced by SL was not explained by obesity or dyslipidemia alone. Therefore, hyperglycemia may be a critical risk factor for fatty acid–induced adipose tissue inflammation. Because palmitic acid is well known to induce inflammation, a diet rich in palmitic acid may aid the elucidation of the mechanism of nutrient-induced adipose tissue inflammation.

The results regarding the adipocyte size and adiponectin level suggested that the accumulation of CD8$^+$ T-cells and M1 macrophages is an essential prerequisite but is not sufficient for adipocyte hypertrophy. The increased expression of E-selectin induced by linoleic acid has been reported in endothelial cells (37), and this might be a similar mechanism of SL-induced E-selectin and P-selectin expression in adipose tissue. Exposure to dietary FFAs on adipose tissue macrophages regulates the expression of PAI-1 (25), but FFA was not increased in this model. The SL diet–induced upregulation of PAI-1 expression might be caused by FFA-independent mechanisms. Linoleic acid is converted to arachidonic acid in vivo, and arachidonic acid is converted to prostaglandins, leukotrienes, and other lipid mediators by lipoxygenase or cyclooxygenase (38). Recently, 5-lipoxygenase, which generates leukotrienes from arachidonic acid, has been reported to induce adipose tissue inflammation (39), and endothelial 15-lipoxygenase and 12/15-lipoxygenase have been reported to be inducers of atherosclerosis via a monocyte-endothelial interaction (40). We noted that the tissue content of arachidonic acid was significantly increased in mice fed an SL diet compared with mice fed an SO diet (E.T. and K.A., unpublished data). The SL diet–induced adipose tissue inflammation may be partly mediated by the increased expression of selectins, the production of PAI-1, or the activation of the arachidonic acid cascade.

Given that a significant difference in body weight gain in the SL-fed *Gck*$^{+/-}$ mice was observed only after week 17, the protective effects of DFS on adipose tissue and the liver were not fully explained by the suppressed body weight gain alone. By contrast, the reduced body weight gain might at least partly be due to a reduction in visceral fat accumulation induced by DFS. DFS reportedly exhibited a significantly reduced body weight gain in high-fat diet–fed mice, but no significant differences in food intake, oxygen consumption, or locomotor activity were observed after chronic DFS administration (20). DPP4-deficient mice also demonstrated a resistance to diet-induced obesity (41). Because clinical data suggest that DPP-4 inhibitors have a neutral effect on body weight (42), the reduced body weight gain by DPP-4 inhibition may be associated with species specificity. Our results suggest that the increased expressions of E-selectin and P-selectin on the SL diet were not required for the DFS-mediated suppression of adipose tissue inflammation, and neither DFS nor GLP-1 directly affected the phase of cytokine production from CD8$^+$ T-cells that mediated macrophage recruitment to the fat tissue. Therefore, DFS might modify the migration of T-cells or the interactions of intercellular adhesion molecules among T-cells, endothelial cells, and stromal cells. The GIP receptor, but not the GLP-1 receptor, is expressed in adipose tissue. Thus, the increase in active GLP-1 arising from DPP-4 inhibition may not stimulate adipocytes directly. Because GIP receptor-deficient mice had a lower weight and a lower adiposity (43), it seems unlikely that the increase in active GIP arising from the inhibition of DPP-4 caused a reduction in visceral fat. Nevertheless, the effects of GIP or other peptides on adipose tissue inflammation remain unclear. DFS may affect certain chemokines whose activities are regulated by DPP-4. The interaction and recruitment of adipose tissue T-cells and macrophages remain controversial. Further study is needed to elucidate the molecular mechanisms of the DFS-mediated prevention of CD8$^+$ T-cells and the M1 macrophage infiltration of adipose tissues, enabling the therapeutic potential of DPP-4 inhibition in adipose tissue to be determined.

The consumption of sucrose or fructose, but not glucose, reportedly induced hepatic de novo lipogenesis, postprandial dyslipidemia, and obesity in both animal models and humans (44–46). In this study, sucrose, rather than fatty acids, played a dominant role in the induction of steatosis because an isocaloric palatinose-rich diet did not induce steatosis. In human hepatocytes, the expressions of GLP-1 receptor and GLP-1 receptor internalization by GLP-1 or exendin-4 have been reported (15); however, GLP-1 receptor expression in the liver has been a controversial issue. A recent study showed that the dephosphorylation of eukaryotic initiation factor 2α by GADD34 in the liver resulted in attenuation of hepatic steatosis (47), raising the possibility that the prevention of liver steatosis by DFS was due to a reduction in endoplasmic reticulum stress in the liver by GLP-1R signaling, similar to the situation in pancreatic β-cells. The effects of sitagliptin on postprandial lipoprotein metabolism may be involved in the

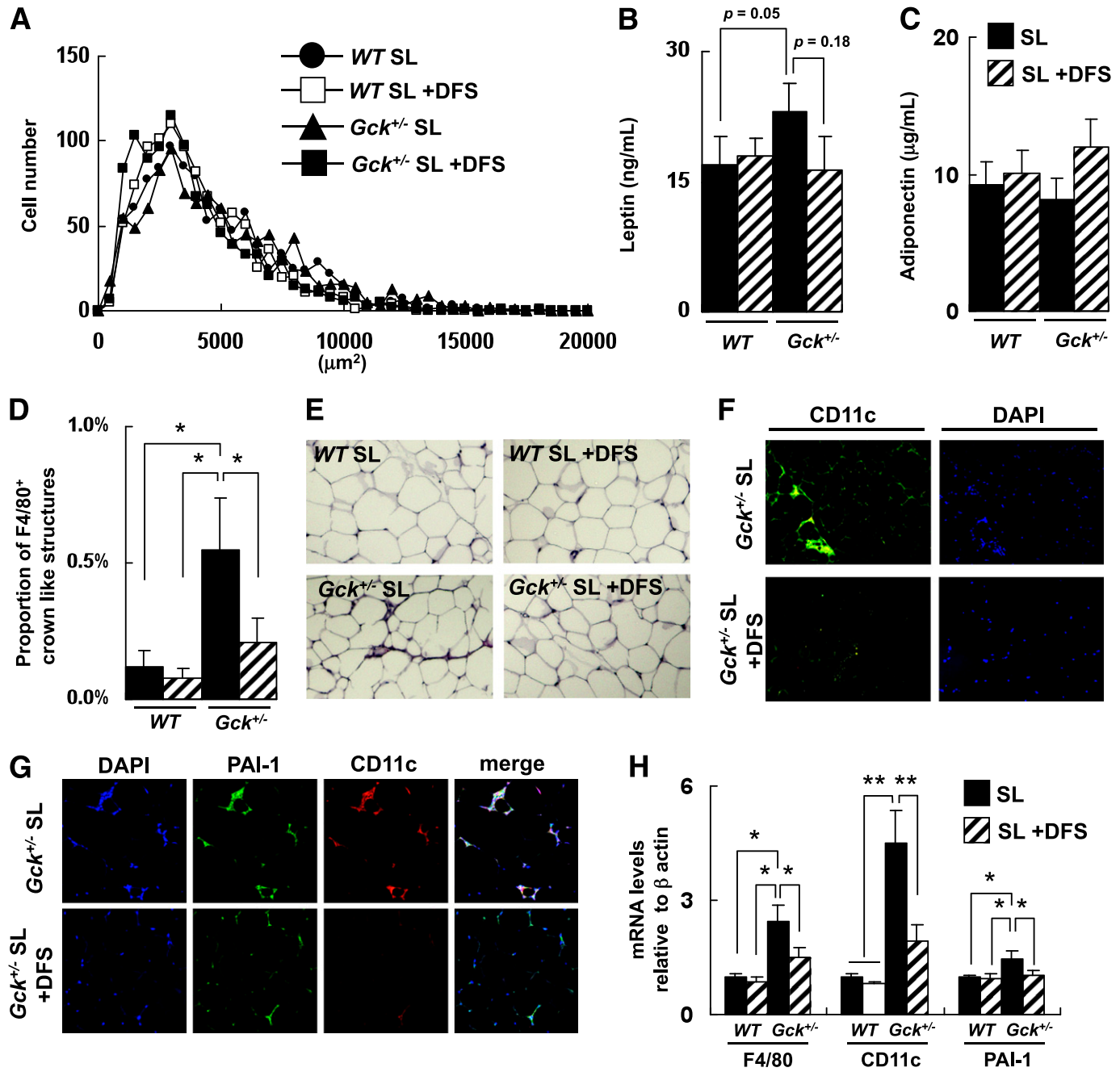

FIG. 5. DFS prevented SL-induced adipose tissue infiltration by M1 macrophages and expression of PAI-1. *A*: Histogram of adipocyte size of the epididymal fat (n = 5). *B* and *C*: Serum leptin and adiponectin levels (n = 6–8). *D* and *E*: Epididymal fat tissue was stained with anti-F4/80 antibody. The number of CLSs was counted as described in RESEARCH DESIGN AND METHODS (n = 5). *F*: Epididymal fat tissue was stained with anti-CD11c antibody and DAPI. *G*: Epididymal fat tissue was stained with anti–PAI-1 antibody and anti-CD11c antibody. Experiments were performed on wild-type (*WT*) and *Gck*$^{+/-}$ mice after 25 weeks on the SO or SL diet. *H*: Assessment of the level of expression of the mRNAs indicated in epididymal fat as determined by real-time quantitative RT-PCR and normalization to the β-actin mRNA level (n = 5). Experiments were performed on wild-type and *Gck*$^{+/-}$ mice after 20 weeks on the SL or the SL-plus-DFS diet. *P < 0.05. **P < 0.01. (A high-quality digital representation of this figure is available in the online issue.)

prevention of fatty liver and the reduction of liver triglycerides (48). The high chronic exposure to insulin can cause peripheral insulin resistance due to the insulin-induced adipogenesis and obesity, whereas insulin resistance also induces steatosis by increased hepatic lipogenesis. In the current study, despite the insulin resistance in liver the mice were insulin sensitive at the whole-body level, and DFS increased hepatic insulin sensitivity by preventing hepatic steatosis and decreasing the expression of PEPCK and G6Pase. Therefore, our results imply the possible involvement of DPP-4 in the complex interplay between adipose tissue and liver in the development of insulin resistance.

In summary, we created a model of nutrient-induced visceral fat inflammation in a diabetic state and showed that DPP-4 inhibition with DFS ameliorated adipose tissue infiltration and NAFLD. Because the biological activities of the large number of chemokines, adipokines, neuropeptides, and incretins are modified by DPP-4–mediated

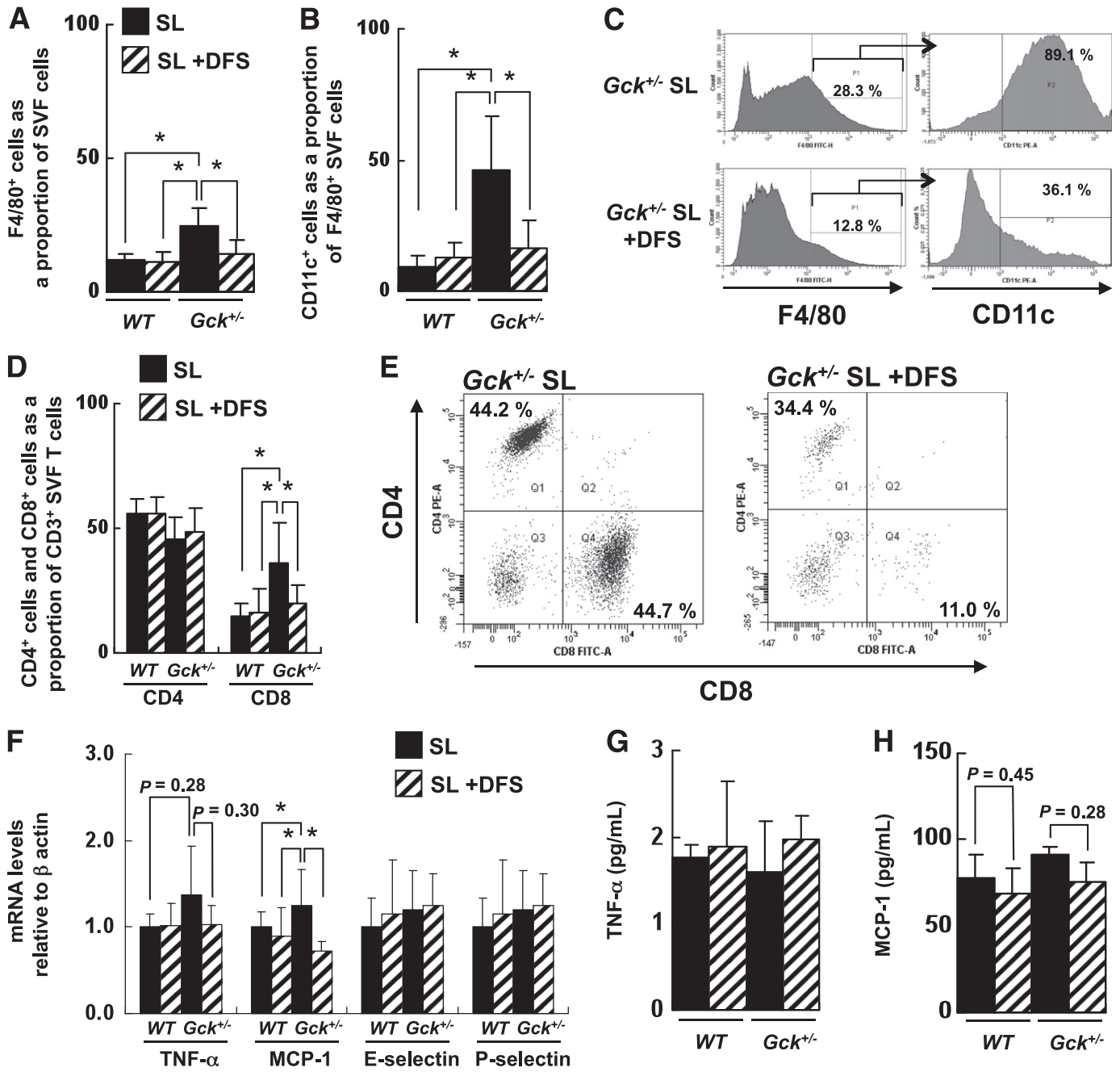

FIG. 6. DFS protected against SL-induced adipose tissue inflammation by infiltration of M1 macrophages and CD8$^+$ T-cells. *A*: Number of F4/80$^+$ cells as a proportion of the cells in the SVF of epididymal fat from the mice as determined by flow cytometry (n = 5). *B*: Number of CD11c$^+$ cells as a proportion of the F4/80$^+$ cells in the SVF of epididymal fat from the groups of mice indicated as determined by flow cytometry (n = 5). *C*: Flow cytometric analysis of CD11c$^+$ cells among F4/80$^+$ SVF cells from the epididymal fat of *Gck*$^{+/-}$ mice. *D* and *E*: Flow cytometric analysis of the CD4$^+$ subset and CD8$^+$ subset of CD3$^+$ T-cells in the epididymal fat of the groups of mice indicated (n = 5). *F*: Assessment of the level of expression of the mRNAs indicated in epididymal fat as determined by real-time quantitative RT-PCR and normalization to the β-actin mRNA level (n = 5). *G* and *H*: Serum TNF-α and MCP-1 levels (n = 6–8). Experiments were performed on wild-type (*WT*) and *Gck*$^{+/-}$ mice after 20 weeks on the SL or the SL-plus-DFS diet. *P < 0.05.

cleavages, the inhibition of DPP-4 might have multiple pleiotrophic effects. The results of the current study demonstrate a novel therapeutic potential of DPP-4 inhibitor for extrapancreatic effects in diabetic patients, but further research is needed to clarify the mechanisms.

ACKNOWLEDGMENTS

This work was supported in part by Grants-in-Aid for Scientific Research (B) 19390251 and (B) 21390282 from the Ministry of Education, Culture, Sports, Science and Technology of Japan, a Medical Award from the Japan Medical Association, a Grant-in-Aid from the Japan Diabetes Foundation, a Grant-in-Aid from the Suzuken Memorial Foundation, a Grant-in-Aid from the Naito Foundation, a Grant-in-Aid from the Uehara Memorial Foundation (to Y.T.), and a Grant-in-Aid for Japan Society for the Promotion of Science fellows (to J.S.).

No potential conflicts of interest relevant to this article were reported.

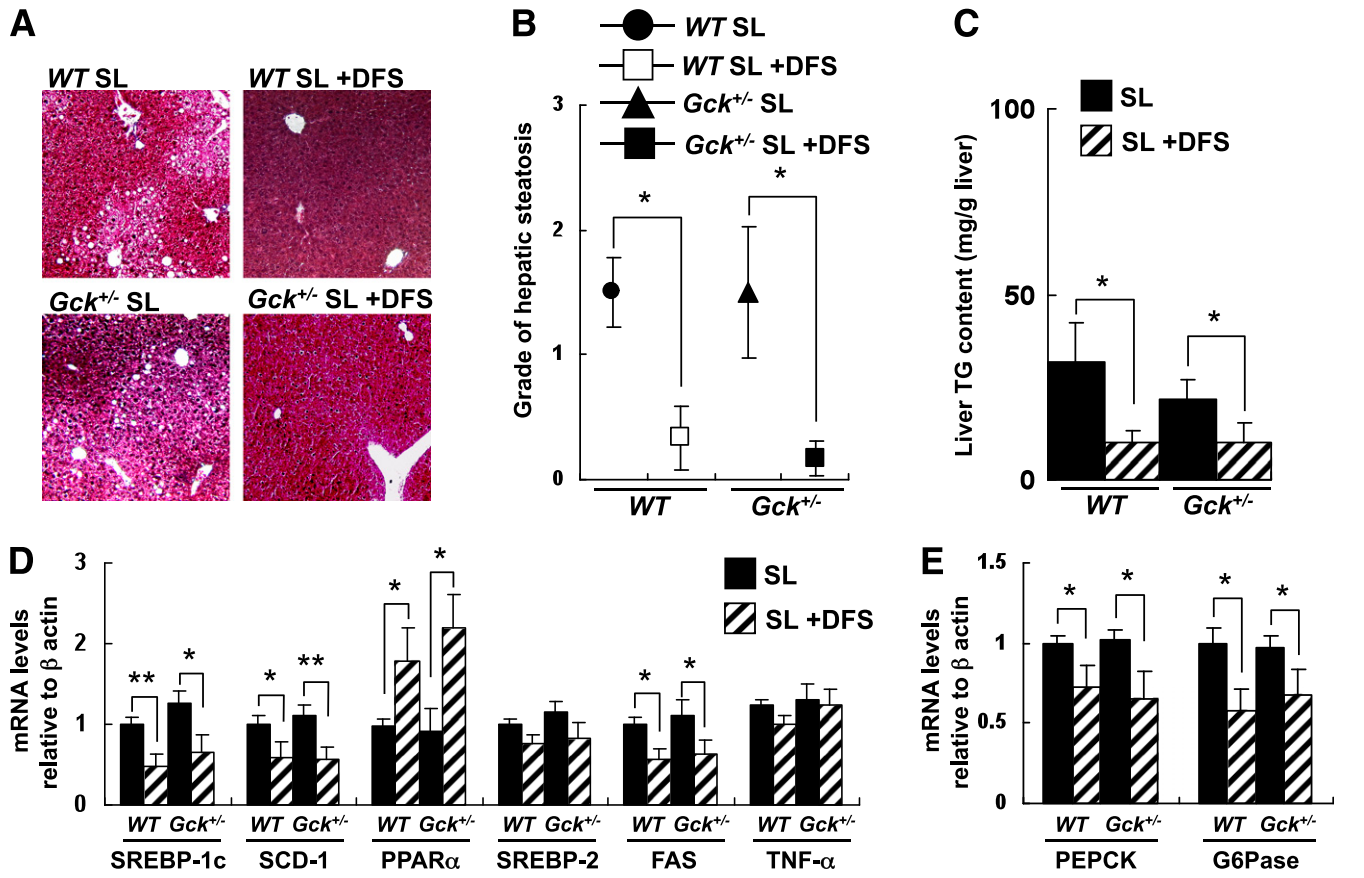

FIG. 7. DFS protected against diet-induced hepatic steatosis. *A*: Masson-Goldner staining of liver sections from the groups of mice indicated. *B*: Grade of hepatic steatosis (grade 0–3) as described in Supplementary Fig. 14 (n = 7). *C*: Concentration of liver triglyceride in the groups of mice indicated (mg/g tissue) (n = 6). *D*: Hepatic gene expression of SREBP-1c, SCD-1, PPARα, SREBP-2, FAS, and TNF-α in the groups of mice indicated normalized to the β-actin mRNA level (n = 6). *E*: Hepatic gene expression of PEPCK and G6Pase in the groups of mice indicated normalized to the β-actin mRNA level (n = 5). Experiments were performed on wild-type (*WT*) and *Gck*$^{+/-}$ mice after 20 weeks on the SL diet or SL-plus-DFS diet. *P < 0.05. **P < 0.01. (A high-quality digital representation of this figure is available in the online issue.)

J.S. researched data, wrote the manuscript, contributed to discussion, and reviewed and edited the manuscript. H.F. researched data and contributed to discussion. K.O., K.S., and Y.I. contributed to discussion. M.K. and E.S. researched data. M.K. and H.S. contributed to discussion. Y.N. researched data and contributed to discussion. K.Am., K.Ao., C.M., and E.T. contributed to discussion. Y.T. wrote the manuscript, reviewed and edited the manuscript, and contributed to discussion.

The authors thank Shigeo Koyasu (Keio University) for his critical reading of the manuscript and for discussion, Naoto Kubota and Takashi Kadowaki (University of Tokyo) for contributing to discussion and providing *Gck*$^{+/-}$ mice, and Misa Katayama (Yokohama City University) for secretarial assistance. The authors thank Merck & Co., Inc. (Rahway, NJ) for providing the DFS and for encouraging their research.

REFERENCES

1. Grundy SM, Abate N, Chandalia M. Diet composition and the metabolic syndrome: what is the optimal fat intake? Am J Med 2002;113(Suppl. 9B): 25S–29S
2. Poitout V, Robertson RP. Glucolipotoxicity: fuel excess and beta-cell dysfunction. Endocr Rev 2008;29:351–366
3. Matsuzawa Y. The role of fat topology in the risk of disease. Int J Obes (Lond) 2008;32(Suppl. 7):S83–S92
4. Neels JG, Olefsky JM. Inflamed fat: what starts the fire? J Clin Invest 2006; 116:33–35
5. Qureshi K, Abrams GA. Metabolic liver disease of obesity and role of adipose tissue in the pathogenesis of nonalcoholic fatty liver disease. World J Gastroenterol 2007;13:3540–3553
6. Hodson L, Skeaff CM, Fielding BA. Fatty acid composition of adipose tissue and blood in humans and its use as a biomarker of dietary intake. Prog Lipid Res 2008;47:348–380
7. Sato K, Arai H, Mizuno A, et al. Dietary palatinose and oleic acid ameliorate disorders of glucose and lipid metabolism in Zucker fatty rats. J Nutr 2007;137:1908–1915
8. Kim D, Wang L, Beconi M, et al. (2R)-4-oxo-4-[3-(trifluoromethyl)-5,6-dihydro[1,2,4]triazolo[4,3-a]pyrazin-7(8H)-yl]-1-(2,4,5-trifluorophenyl)butan-2-amine: a potent, orally active dipeptidyl peptidase IV inhibitor for the treatment of type 2 diabetes. J Med Chem 2005;48:141–151
9. Xu G, Stoffers DA, Habener JF, Bonner-Weir S. Exendin-4 stimulates both beta-cell replication and neogenesis, resulting in increased beta-cell mass and improved glucose tolerance in diabetic rats. Diabetes 1999;48:2270–2276
10. Farilla L, Hui H, Bertolotto C, et al. Glucagon-like peptide-1 promotes islet cell growth and inhibits apoptosis in Zucker diabetic rats. Endocrinology 2002;143:4397–4408
11. Ahrén B. GLP-1 and extra-islet effects. Horm Metab Res 2004;36:842–845
12. Verge D, López X. Impact of GLP-1 and GLP-1 receptor agonists on cardiovascular risk factors in type 2 diabetes. Curr Diabetes Rev 2010;6:191–200
13. Ding X, Saxena NK, Lin S, Gupta NA, Anania FA. Exendin-4, a glucagon-like protein-1 (GLP-1) receptor agonist, reverses hepatic steatosis in ob/ob mice. Hepatology 2006;43:173–181
14. Lee YS, Shin S, Shigihara T, et al. Glucagon-like peptide-1 gene therapy in obese diabetic mice results in long-term cure of diabetes by improving insulin sensitivity and reducing hepatic gluconeogenesis. Diabetes 2007;56: 1671–1679
15. Gupta NA, Mells J, Dunham RM, et al. Glucagon-like peptide-1 receptor is present on human hepatocytes and has a direct role in decreasing hepatic

steatosis in vitro by modulating elements of the insulin signaling pathway. Hepatology 2010;51:1584–1592
16. Arakawa M, Mita T, Azuma K, et al. Inhibition of monocyte adhesion to endothelial cells and attenuation of atherosclerotic lesion by a glucagon-like peptide-1 receptor agonist, exendin-4. Diabetes 2010;59:1030–1037
17. Hadjiyanni I, Siminovitch KA, Danska JS, Drucker DJ. Glucagon-like peptide-1 receptor signalling selectively regulates murine lymphocyte proliferation and maintenance of peripheral regulatory T cells. Diabetologia 2010;53:730–740
18. Terauchi Y, Sakura H, Yasuda K, et al. Pancreatic beta-cell-specific targeted disruption of glucokinase gene. Diabetes mellitus due to defective insulin secretion to glucose. J Biol Chem 1995;270:30253–30256
19. Terauchi Y, Takamoto I, Kubota N, et al. Glucokinase and IRS-2 are required for compensatory beta cell hyperplasia in response to high-fat diet-induced insulin resistance. J Clin Invest 2007;117:246–257
20. Lamont BJ, Drucker DJ. Differential antidiabetic efficacy of incretin agonists versus DPP-4 inhibition in high fat fed mice. Diabetes 2008;57:190–198
21. Lumeng CN, Bodzin JL, Saltiel AR. Obesity induces a phenotypic switch in adipose tissue macrophage polarization. J Clin Invest 2007;117:175–184
22. Shirakawa J, Wang Y, Tahara-Hanaoka S, Honda S, Shibuya K, Shibuya A. LFA-1-dependent lipid raft recruitment of DNAM-1 (CD226) in CD4+ T cell. Int Immunol 2006;18:951–957
23. Ohnuma K, Yamochi T, Uchiyama M, et al. CD26 up-regulates expression of CD86 on antigen-presenting cells by means of caveolin-1. Proc Natl Acad Sci USA 2004;101:14186–14191
24. Cinti S, Mitchell G, Barbatelli G, et al. Adipocyte death defines macrophage localization and function in adipose tissue of obese mice and humans. J Lipid Res 2005;46:2347–2355
25. Kishore P, Li W, Tonelli J, et al. Adipocyte-derived factors potentiate nutrient-induced production of plasminogen activator inhibitor-1 by macrophages. Sci Transl Med 2010;2:20ra15
26. Nishimura S, Manabe I, Nagasaki M, et al. CD8+ effector T cells contribute to macrophage recruitment and adipose tissue inflammation in obesity. Nat Med 2009;15:914–920
27. Kintscher U, Hartge M, Hess K, et al. T-lymphocyte infiltration in visceral adipose tissue: a primary event in adipose tissue inflammation and the development of obesity-mediated insulin resistance. Arterioscler Thromb Vasc Biol 2008;28:1304–1310
28. Rausch ME, Weisberg S, Vardhana P, Tortoriello DV. Obesity in C57BL/6J mice is characterized by adipose tissue hypoxia and cytotoxic T-cell infiltration. Int J Obes (Lond) 2008;32:451–463
29. Nishimura S, Manabe I, Nagasaki M, et al. In vivo imaging in mice reveals local cell dynamics and inflammation in obese adipose tissue. J Clin Invest 2008;118:710–721
30. Ohnuma K, Dang NH, Morimoto C. Revisiting an old acquaintance: CD26 and its molecular mechanisms in T cell function. Trends Immunol 2008;29:295–301
31. Ohnuma K, Munakata Y, Ishii T, et al. Soluble CD26/dipeptidyl peptidase IV induces T cell proliferation through CD86 up-regulation on APCs. J Immunol 2001;167:6745–6755
32. Anstee QM, Goldin RD. Mouse models in non-alcoholic fatty liver disease and steatohepatitis research. Int J Exp Pathol 2006;87:1–16
33. Feldstein AE, Canbay A, Guicciardi ME, Higuchi H, Bronk SF, Gores GJ. Diet associated hepatic steatosis sensitizes to Fas mediated liver injury in mice. J Hepatol 2003;39:978–983
34. Eliassen KA, Brodal BP, Svindland A, et al. Activity of peroxisomal enzymes, and levels of polyamines in LPA-transgenic mice on two different diets. Lipids Health Dis 2005;4:23
35. Gustafson B, Hammarstedt A, Andersson CX, Smith U. Inflamed adipose tissue: a culprit underlying the metabolic syndrome and atherosclerosis. Arterioscler Thromb Vasc Biol 2007;27:2276–2283
36. Sumiyoshi M, Sakanaka M, Kimura Y. Chronic intake of high-fat and high-sucrose diets differentially affects glucose intolerance in mice. J Nutr 2006;136:582–587
37. Saraswathi V, Wu G, Toborek M, Hennig B. Linoleic acid-induced endothelial activation: role of calcium and peroxynitrite signaling. J Lipid Res 2004;45:794–804
38. Schmitz G, Ecker J. The opposing effects of n-3 and n-6 fatty acids. Prog Lipid Res 2008;47:147–155
39. Horrillo R, González-Périz A, Martínez-Clemente M, et al. 5-lipoxygenase activating protein signals adipose tissue inflammation and lipid dysfunction in experimental obesity. J Immunol 2010;184:3978–3987
40. Hatley ME, Srinivasan S, Reilly KB, Bolick DT, Hedrick CC. Increased production of 12/15 lipoxygenase eicosanoids accelerates monocyte/endothelial interactions in diabetic db/db mice. J Biol Chem 2003;278:25369–25375
41. Conarello SL, Li Z, Ronan J, et al. Mice lacking dipeptidyl peptidase IV are protected against obesity and insulin resistance. Proc Natl Acad Sci USA 2003;100:6825–6830
42. Ahrén B. Dipeptidyl peptidase-4 inhibitors: clinical data and clinical implications. Diabetes Care 2007;30:1344–1350
43. Miyawaki K, Yamada Y, Ban N, et al. Inhibition of gastric inhibitory polypeptide signaling prevents obesity. Nat Med 2002;8:738–742
44. Lê KA, Tappy L. Metabolic effects of fructose. Curr Opin Clin Nutr Metab Care 2006;9:469–475
45. Bizeau ME, Pagliassotti MJ. Hepatic adaptations to sucrose and fructose. Metabolism 2005;54:1189–1201
46. Stanhope KL, Schwarz JM, Keim NL, et al. Consuming fructose-sweetened, not glucose-sweetened, beverages increases visceral adiposity and lipids and decreases insulin sensitivity in overweight/obese humans. J Clin Invest 2009;119:1322–1334
47. Oyadomari S, Harding HP, Zhang Y, Oyadomari M, Ron D. Dephosphorylation of translation initiation factor 2alpha enhances glucose tolerance and attenuates hepatosteatosis in mice. Cell Metab 2008;7:520–532
48. Hsieh J, Longuet C, Baker CL, et al. The glucagon-like peptide 1 receptor is essential for postprandial lipoprotein synthesis and secretion in hamsters and mice. Diabetologia 2010;53:552–561